

Bed Deformation Characteristics at Confluence of Rivers Which Have Different Cohesive Characteristics of Sediment

Hiroshi TAKEBAYASHI, Puji HARSANTO⁽¹⁾, NGUYEN Manh Minh Toan⁽¹⁾
and Masaharu FUJITA

(1) Graduate School of Engineering, Kyoto University

Synopsis

The depth integrated two dimensional bed deformation analysis has been performed to understand the seasonal change of the flow pattern, bed deformation characteristics and horizontal distribution characteristics of bed material size. Furthermore, the bed material is treated as both the cohesive and the non-cohesive sediments and the effect of the horizontal distribution of cohesive material on bed deformation characteristics is discussed. The result shows that the sediment deposited at the south of the peninsula between the Tonle Sap River and the Mekong River during the flood season. The peninsula between the Tonle Sap River and the Mekong River has been extended to south year by year. The sediment deposition during the flood season causes the extension of the peninsula. Furthermore, cohesive characteristics of the sediment affects the bed deformation characteristics because of the suppression of sediment transport rate and bed degradation. Especially, when rivers which have different sediment size characteristics confluents, difference of the cohesive characteristics of the sediment must be considered.

Keywords: cohesive material, numerical analysis, Chaktomuk, confluence

1. Introduction

Chaktomuk, which is the confluence and diversion area among the Mekong River, the Tonle Sap River and the Bassac River, is located in the north part of the Mekong Delta as shown in Figure 1. The Mekong River changes its flow from west to east at Phnom Penh, where the two rivers, the Tonle Sap River and the Bassac River, diverge. There is the Tonle Sap Lake at the north boundary of the Tonle Sap River. The Tonle Sap Lake is the largest freshwater storage in the Southeast Asia, which covers an area of about 13000 km² [1]. The Tonle Sap flow system is well known because of its unique hydrological regime and its contribution to both the economy and the

ecosystem of Cambodia and South Vietnam. A unique hydrological system of the river is the inverse flow that takes place from June to September. In June, the water in the Mekong River starts to flow to the Tonle Sap River because of the flood in the Mekong River. Thus, the river flow begins to enter the lake and the Tonle Sap Lake behaves as an effective flood detention basin. On the other hand, from October to May, the flow direction in the Tonle Sap River is from the Tonle Sap Lake to the Mekong River because of the decreasing of the water surface elevation in the Mekong River. In this stage, the lake plays as a water supplier to the downstream area of the Mekong River.

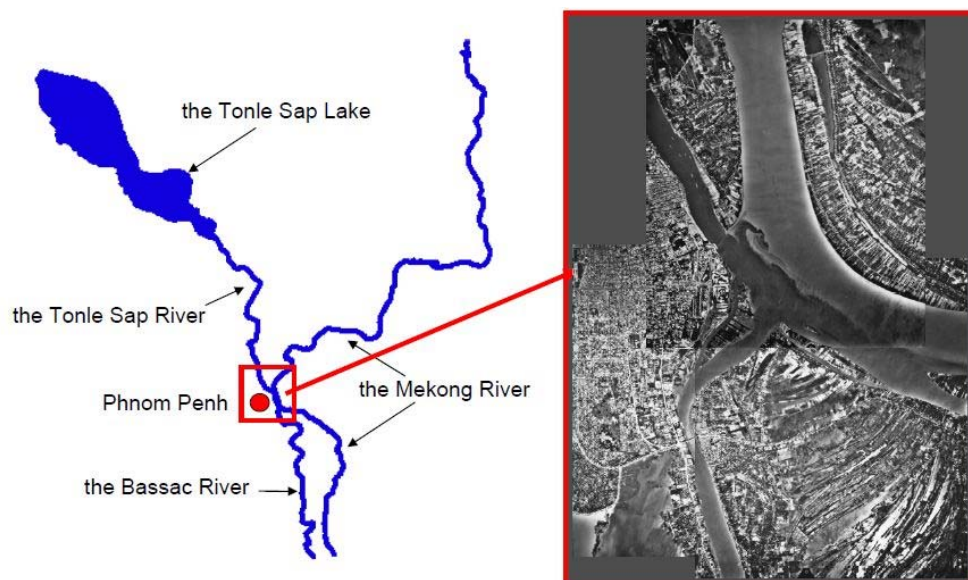


Figure 1 Location of Chaktomuk

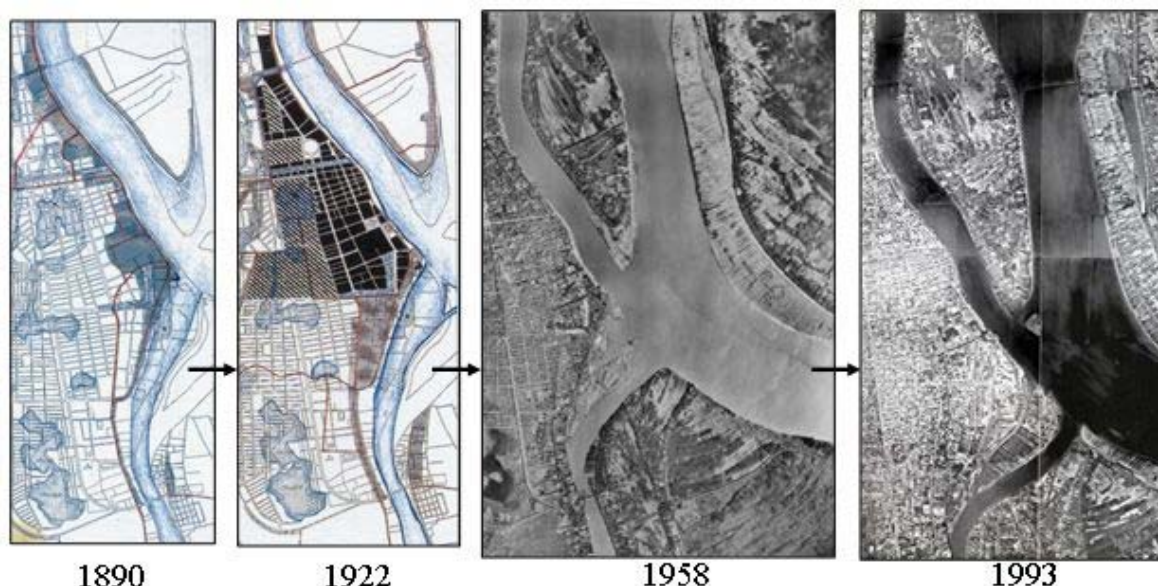


Figure 2 Temporal change of channel geometry of Chaktomuk (figs of 1890, 1922 and photo in 1993 is from *Ministere de la Culture : Phnom Penh, development urban et patrimoine*, photo in 1958 is from *Ministry of Industry, Mines and Energy General Department of Mineral Resources, Phnom Penh, Cambodia*)

Both bed and bank deformation at Chaktomuk has been occurred with the complex flow. The morphological deformation can change the flow characteristics at Chaktomuk and must be assessed on both the channel form and the flow characteristics for the economy and the ecosystem of both Cambodia and South Vietnam. K. W. Olsen and S. Tjerry [2] performed the two dimensional bed deformation analysis of Chaktomuk area and suggested the river regulation works to suppress bank erosions. This study must be a great job and give us much information. However, in the analysis, bed material is treated as uniform sediment. The mean diameter of

the bed material in Tonle Sap River is quite difference from that in Mekong River: the bed material in Tonle Sap River is fine that in the Mekong River is coarse. H. Takebayashi et al. [3] treats the bed material as the non-uniform sediment and clarify the effect of the sediment size distribution on the bed deformation characteristics and the horizontal distribution characteristics of the sediment size. On the other hand, the bed material in Tonle Sap River consists of cohesive material. It is considered that the cohesive characteristic of the bed material affects the horizontal distribution of bed deformation very well.

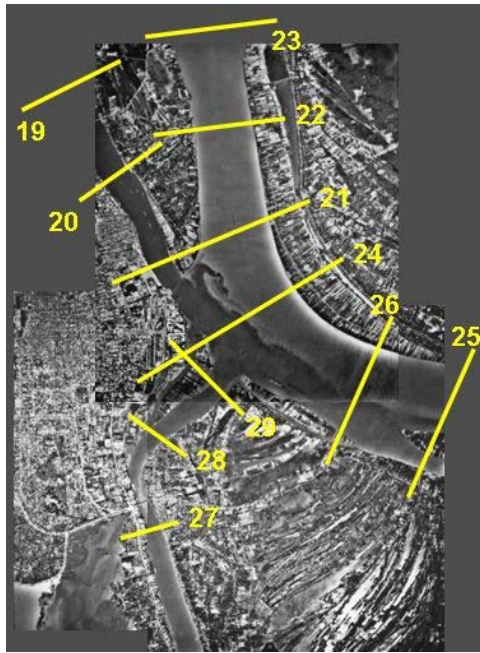
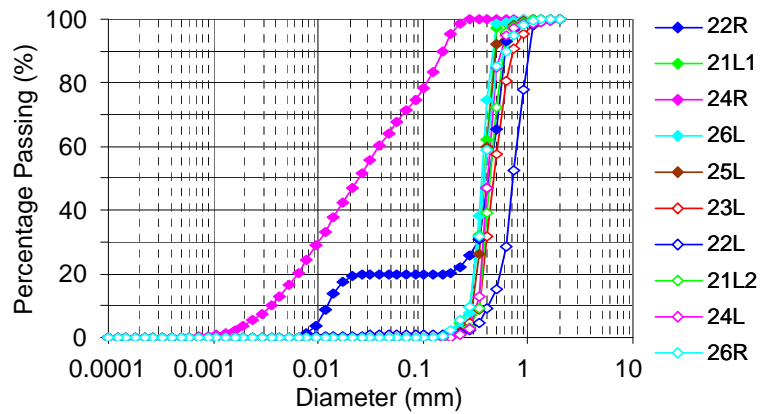
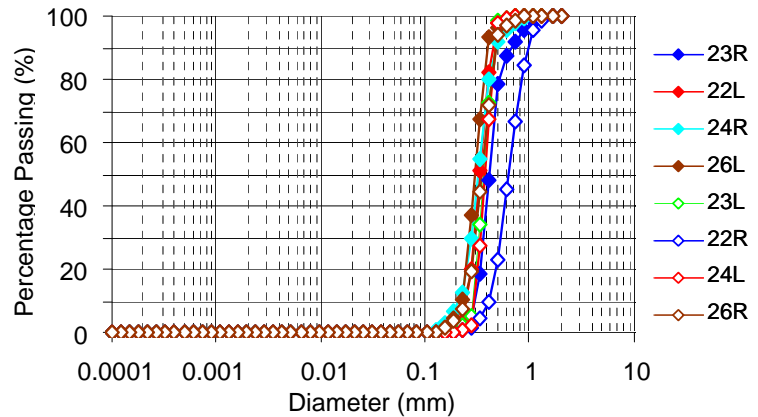


Figure 3 Sampled cross-sections of bed and bank materials



(a) Dry season (February 2005)



(b) Flood season (September 2005)

Figure 4 Size distribution of bed material in Chaktomuk

In this study, the depth integrated two dimensional bed deformation analysis has been performed to understand the seasonal change of the flow pattern, bed deformation characteristics and horizontal distribution characteristics of bed material size. In the analysis, bed material is treated as both the cohesive and the non-cohesive sediments and the effect of the horizontal distribution of cohesive material on bed deformation characteristics is discussed. The analysis is performed under 3 hydraulic conditions; maximum, minimum and zero water discharge in the Tonle Sap River.

2. Field survey

Bed materials were sampled at two points in a cross-section using a cable operated sediment sampler during both flood and dry seasons (H. Takebayashi et al., 2010). The sampler can take the sediment in 8cm thickness from the bed surface. Sediment is also sampled from both the left and the right banks. Figure 3 shows the sampling cross-sections of bed and bank materials.

Figure 4 shows the size distribution of bed

material around the Chaktomuk. The size distribution of the bed material during flood has a small spatial change and their mean diameter is coarse. But the mean diameter of the bed material during dry season distributes in wide range; finer sediment is included in the data. During dry season, flow direction in the Tonle Sap River is from north to south (from the Tonle Sap Lake to the Mekong River) and the water discharge in the Tonle Sap River is large. The aerial photo in Figure 1 is taken during dry seasons. The line due to the large difference of sediment concentration is observed in the confluence between the Tonle Sap River and the Mekong River. This photo indicates that the Tonle Sap River supplies fine sediment to both the Mekong River and the Bassac River during dry season. In other words, seasonal change of flow direction in the Tonle Sap River contributes to the seasonal change of the sediment size around Chaktomuk.

3. Numerical analysis

3.1 Governing equations

Computation of the water flow is performed using

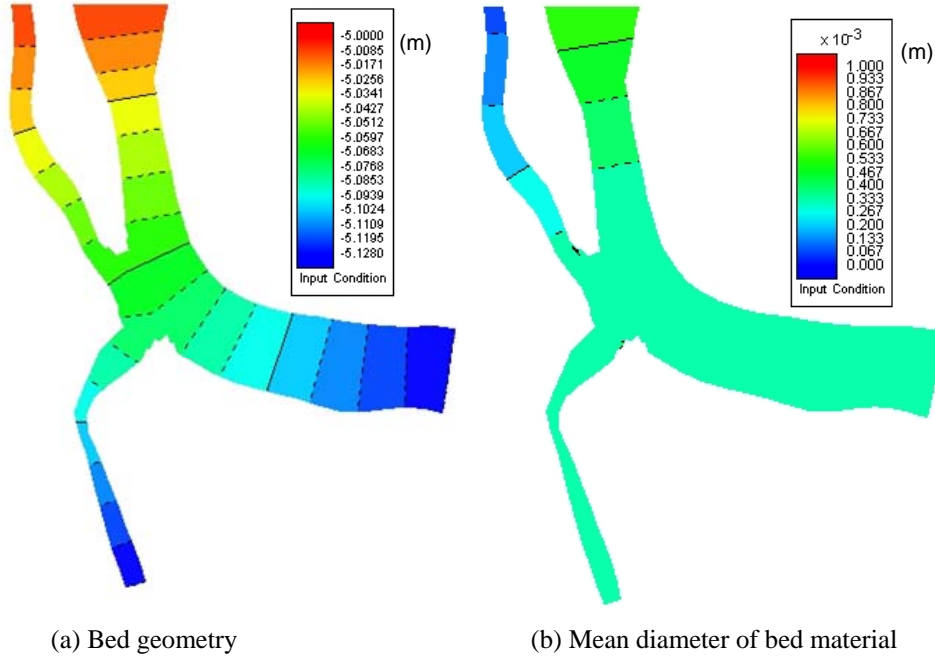


Figure 5 Initial bed geometry and horizontal distribution of initial mean diameter of bed material (Channel geometry: 1993)

the governing equation of the horizontal two dimensional flow averaged with depth [4]. Equations in the model are written in the general coordinate system. Grain size distribution is evaluated using the following mass conservation equation of each sediment size class:

$$\begin{aligned} & \frac{\partial}{\partial t} \left(\frac{c_b E_b f_{bk}}{J} \right) + (1-\lambda) F_{bk} \frac{\partial}{\partial t} \left(\frac{z_b}{J} \right) \\ & + \frac{\partial}{\partial \xi} \left(\frac{q_{b\xi k}}{J} \right) + \frac{\partial}{\partial \eta} \left(\frac{q_{b\eta k}}{J} \right) + \frac{1}{J} w_k (c_{sbe k} - c_{sbk}) = 0 \\ & \begin{cases} F_{bk} = f_{d1k}, \partial z_b / \partial t \leq 0 \\ F_{bk} = f_{bk}, \partial z_b / \partial t \geq 0 \end{cases} \quad (1) \end{aligned}$$

$$\begin{aligned} & \frac{\partial}{\partial t} \left(\frac{E_{d1} f_{d1k}}{J} \right) - F_{dk} \frac{\partial}{\partial t} \left(\frac{E_{d1}}{J} \right) = 0 \\ & \begin{cases} F_{dk} = f_{d1k}, \partial z_b / \partial t \leq 0 \\ F_{dk} = f_{bk}, \partial z_b / \partial t \geq 0 \end{cases} \quad (2) \end{aligned}$$

In the formulae above, f_{bk} is the concentration of bed load of size class k in the bed load layer, f_{dmk} is the sediment concentration of size class k in the m th bed layer, c_b is the depth-averaged concentration of bed load. E_b is the bed load layer thickness, $q_{b\xi k}$ and $q_{b\eta k}$ are the bed load of size class k in ξ and η directions, respectively, q_{bxk} and q_{byk} are the bed load of size class k in x and y directions, respectively as follows [5], [6],

[7].

$$q_{bxk} = q_{bk} \cos \beta_k, \quad q_{byk} = q_{bk} \sin \beta_k \quad (3)$$

$$q_{bk} = 17 \frac{\rho u_{*e}^3}{(\rho_s - \rho) g} \left(1 - \sqrt{K_c} \frac{u_{*ck}}{u_*} \right) \left(1 - K_c \frac{u_{*ck}^2}{u_*^2} \right) f_{bk} \quad (4)$$

Therein, ρ_s is the sediment density, u_{*e} is the effective shear velocity, the non-dimensional critical friction velocity of size class k is evaluated as follows [5].

$$u_{*ck}^2 = u_{*cm}^2 \left[\frac{\log_{10} 19}{\log_{10} (19 d_k / d_m)} \right]^2 \frac{d_k}{d_m} \quad d_k / d_m \geq 0.4 \quad (5)$$

$$u_{*ck}^2 = 0.85 u_{*cm}^2 \quad d_k / d_m \leq 0.4 \quad (6)$$

Iwagaki's formula [8] which is formulated for uniform bed material is used for evaluating u_{*cm} . K_c is the correction factor due to the influence of bed inclination on sediment motion.

$$K_c = 1 + \frac{1}{\mu_s} \left[\left(\frac{1}{s} + 1 \right) \cos \alpha \tan \theta_x + \sin \alpha \tan \theta_y \right] \quad (7)$$

where s is the specific gravity of the sediment in water, α is the angle of deviation of near-bed flow from the x direction. μ_s is the coefficient of static friction. θ_x and θ_y are bed inclinations in x and y directions, respectively. The deviation angle of bed

Table 1 Hydraulic conditions

	Channel geometry	QmekongU (m ³ /s)	Qtonle (m ³ /s)	Bed material
Case 1	1993	6000	8000	Cohesive
Case 2	1993	20000	0	Cohesive
Case 3	1993	36000	-8000	Cohesive
Case 4	1993	6000	8000	Non-cohesive
Case 5	1993	20000	0	Non-cohesive
Case 6	1993	36000	-8000	Non-cohesive

load of size class k to the x direction (β_k), which depends on the flow near bed and inclination of the bed, is calculated by the following relation.

$$\tan \beta_k = \frac{\sin \alpha - \Pi \Theta_y \left(\frac{u_{*ck}^2}{u_*^2} \right) \tan \theta_y}{\cos \alpha - \Pi \Theta_x \left(\frac{u_{*ck}^2}{u_*^2} \right) \tan \theta_x} \quad (8)$$

$$\Pi = K_{ld} + 1/\mu_s \quad (9)$$

$$\Theta_y = \frac{1}{1 + \tan^2 \theta_x + \tan^2 \theta_y} \quad (10)$$

$$\Theta_x = \Theta_y + \frac{\rho}{\rho_s - \rho} \cos^2 \theta_x \quad (11)$$

where, K_{ld} is the ratio of lift force to drag force. The settling velocity of suspended sediment (w_{fk}) is estimated as follow [9].

$$w_{fk} = \left(\sqrt{\frac{2}{3} + \frac{36v^2}{sgd_k^3}} - \sqrt{\frac{36v^2}{sgd_k^3}} \right) \sqrt{sgd_k} \quad (12)$$

The equilibrium suspended concentration of k sediment size class at reference level (c_{sbek}) is evaluated as follows [10].

$$c_{sbek} = 5.55 \left(\frac{1}{2} \frac{u_*}{w_{fk}} \exp \left(-\frac{w_{fk}}{u_*} \right) \right)^{1.61} f_{bk} \quad (\text{unit: ppm}) \quad (13)$$

When the vertical distribution of concentration of suspended sediment is supposed as exponent distribution, relationship between the depth-averaged suspended concentration (c_{sk}) and the suspended concentration of sediment size class k at reference level (c_{sbk}) is as follows.

$$c_{sk} = \frac{c_{sbk}}{\beta_{sk}} \left(1 - e^{(-\beta_{sk})} \right), \quad \beta_{sk} = \frac{w_{fk} h}{D_h} \quad (14)$$

where, D_h is the coefficient of dispersion in vertical direction. v is used as D_h here for simplicity. The depth-averaged suspended concentration of size class

k is evaluated the following continuum equation of suspended sediment.

$$\begin{aligned} \frac{\partial}{\partial t} \left(\frac{hc_{sk}}{J} \right) + \frac{\partial}{\partial \xi} \left(\frac{hc_{sk}U}{J} \right) + \frac{\partial}{\partial \eta} \left(\frac{hc_{sk}V}{J} \right) \\ = \frac{1}{J} w_{fk} (c_{sbek} - c_{sbk}) \\ + \frac{\partial}{\partial \xi} h \left(\frac{1}{J} \left(D_x \left(\frac{\partial \xi}{\partial x} \right)^2 + D_y \left(\frac{\partial \xi}{\partial y} \right)^2 \right) \frac{\partial c_{sk}}{\partial \xi} \right) \\ + \frac{\partial}{\partial \xi} h \left(\frac{1}{J} \left(D_x \frac{\partial \xi}{\partial x} \frac{\partial \eta}{\partial x} + D_y \frac{\partial \xi}{\partial y} \frac{\partial \eta}{\partial y} \right) \frac{\partial c_{sk}}{\partial \eta} \right) \\ + \frac{\partial}{\partial \eta} h \left(\frac{1}{J} \left(D_x \frac{\partial \xi}{\partial x} \frac{\partial \eta}{\partial x} + D_y \frac{\partial \xi}{\partial y} \frac{\partial \eta}{\partial y} \right) \frac{\partial c_{sk}}{\partial \xi} \right) \\ + \frac{\partial}{\partial \eta} h \left(\frac{1}{J} \left(D_x \left(\frac{\partial \eta}{\partial x} \right)^2 + D_y \left(\frac{\partial \eta}{\partial y} \right)^2 \right) \frac{\partial c_{sk}}{\partial \eta} \right) \end{aligned} \quad (15)$$

where, D_x and D_y are coefficient of dispersion in x and y directions, respectively. ($D_x = D_y = v$ for simplicity here). Evolution of bed elevation is estimated by means of following formulae.

$$\begin{aligned} \frac{\partial}{\partial t} \left(\frac{c_b E_b}{J} \right) + (1 - \lambda) \frac{\partial}{\partial t} \left(\frac{z_b}{J} \right) \\ + \frac{\partial}{\partial \xi} \left(\sum_{k=1}^n \frac{q_{b\zeta k}}{J} \right) + \frac{\partial}{\partial \eta} \left(\sum_{k=1}^n \frac{q_{b\eta k}}{J} \right) \\ + \sum_{k=1}^n \frac{1}{J} w_k (c_{sbek} - c_{sbk}) = 0 \end{aligned}$$

$$E_{sd} \geq E_{be} \frac{c_b}{1 - \lambda} \quad (16)$$

$$\frac{\partial}{\partial t} \left(\frac{z_b}{J} \right) + \frac{V_e}{J} = 0 \quad E_{sd} \leq E_{be} \frac{c_b}{1 - \lambda} \quad (17)$$

In them, n represents the number of the size class of sediment. The erosion velocity of cohesive sediment (V_e) is estimated as follows [11].

Table 2 Water discharge in each channel

	QmekongU (m ³ /s)	Qtonle (m ³ /s)	QmekongD (m ³ /s)	Qbassac (m ³ /s)	Qbassac /QmekongD
Case 1	6000	8000	11133	2867	0.258
Case 2	20000	0	17859	2141	0.120
Case 3	36000	-8000	22687	5313	0.234

$$V_e = \alpha_c R_{wc}^{2.5} u_*^3 (1 - r_b) \quad (18)$$

where, α_c is the coefficient related on kinds of cohesive sediment, R_{wc} is the water content rate. Local bed slope was reset to the angle of repose at calculation points where the slope becomes steeper than the angle of repose [12] and E_{sd} is thicker than E_{be} at the upper erosion area.

3.2 Hydraulic conditions

Table 1 show the hydraulic conditions used in the analysis. Three kinds of flow pattern are used here. In Cases 1 and 4, water discharge in the Tonle Sap River is 8000m³/s. This is the annual maximum water discharge in the Tonle Sap River and can be observed during the dry season. In Cases 2 and 5, water discharge in the Tonle Sap River is 0m³/s. This water discharge can be observed between the dry season and the flood season. In Cases 3 and 6, water discharge in the Tonle Sap River is -8000m³/s. This is the annual minimum water discharge in the Tonle Sap River and can be observed during flood season. Figure 5 (a) show the initial bed geometry. Flat bed geometry with the constant longitudinal slop is used as initial bed geometry to clarify the bed deformation characteristics. Figure 5 (b) shows the initial size distribution of bed material. At the upstream boundary of the Mekong River, the coarse bed material which is measured in the Mekong River is used as the initial sediment size. At the north boundary of the Tonle Sap River, the fine bed material which is measured in the Tonle Sap River is used as the initial sediment size. In the Bassac River and the downstream of the Mekong River, the average size distribution of bed material between the Mekong's material and the Tonle Sap's material is used as the initial condition. In Cases 1, 2 and 3, surface and subsurface bed materials are treated as the non-cohesive and the cohesive materials in the Tonle Sap River, respectively. The thickness of the surface non-cohesive material layer is distributed linearly from 0 to 0.3m along the river. The thickness of the surface non-cohesive material layer is 0 at the

upstream boundary of the Tonle Sap River and is 0.3m at the connection between the Tonle Sap River and the confluence. In the other areas, there is no cohesive material. Both the surface and the subsurface bed materials are treated as non-cohesive material in Cases 4, 5 and 6 to discuss the effect of the horizontal distribution of cohesive material on bed deformation characteristics by comparing the results in Cases 1, 2 and 3.

4. Results and discussion

4.1 Flow characteristics

Figure 6 show the horizontal distributions of the depth averaged water velocity in Cases 1, 2 and 3. Table 2 shows the water discharges of each river. During the dry season (Figure 6 (a)), water discharge in Tonle Sap River is larger than that in the upstream area of the Mekong River. As shown in Table 2, water discharge in the Bassac River is smaller than that in the downstream area of the Mekong River. The percentage rate of the water discharge in the Bassac River to the Mekong River is 25.8%. Hence, the water from the Tonle Sap River diverged to both the Bassac River and the downstream area of the Mekong River during dry season.

When water discharge in the Tonle Sap is zero (Figure 6 (b)), the percentage rate of the water discharge in the Bassac River to the Mekong River is 12.0% and is the minimum value among Cases 1, 2 and 3. Between the entrance of the Bassac River and the Mekong main channel, the very small water velocity area is appear because of the zero water discharge in the Tonle Sap River. Hence, the water in the upstream area of the Mekong River is hard to flow into the Bassac River.

During the flood season (Figure 6 (c)), the water from the upstream area of the Mekong River flows into the Tonle Sap River. Furthermore, the water from the upstream area of the Mekong River tends to flow into the Bassac River, because the flow direction from the upstream area of the Mekong River is changed almost 180 degree at the entrance of the Bassac River.

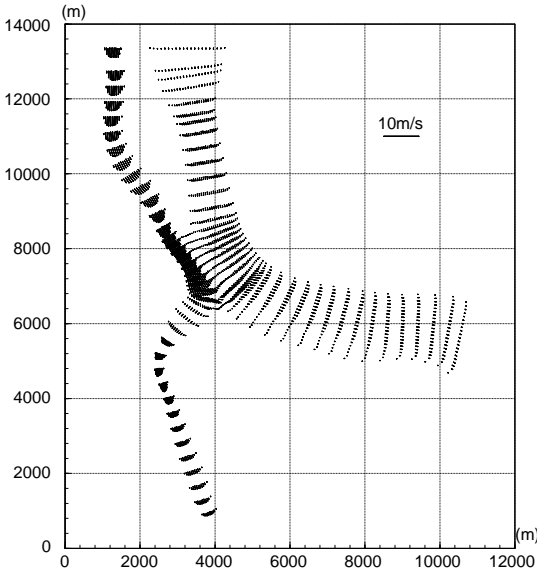
The percentage rate of the water discharge in the Bassac River to the Mekong River is 23.4% and is slightly smaller than that during the dry season.

4.2 Bed deformation and sediment size characteristics

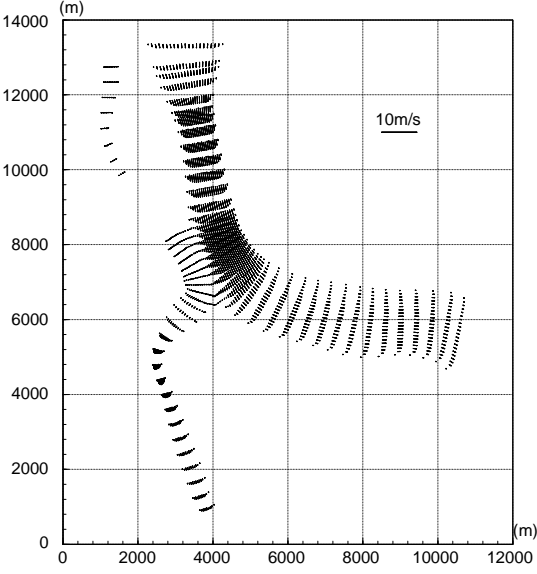
The bed near the confluence in the Tonle Sap River is eroded well during the dry season (Figure 7 (a)). Sediment deposited at the entrance of the Bassac River. The photo in Figure 1 was taken during the dry season. In the photo, the sediment concentration boundary is appeared from the left bank of the Tonle Sap River to the downstream reach of the Mekong River. The photo indicates that the sediment and the water in the Tonle Sap River are supplied to the confluence and the Bassac River very well during the dry season. The calculated results show the same tendency. Bed materials at the bed degradation area become coarse and those at the bed aggradation area become fine as shown in Figure 8 (a).

When water discharge in the Tonle Sap River is zero (Figure 7 (b)), the upstream and the downstream areas of the Mekong River and the Bassac River is degraded. Hence, as shown in Figure 8 (b), the sediment size becomes coarse at the upstream and the downstream areas of the Mekong River and the Bassac River. Sediment deposits near the bifurcation between the Mekong River and the Bassac River.

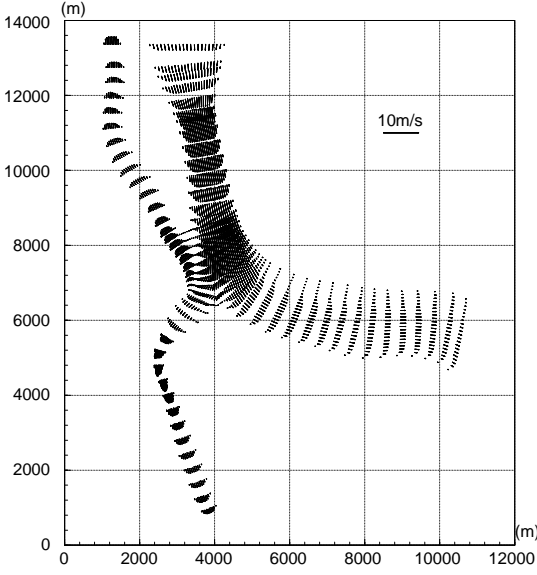
During the flood season (Figure 7 (c)), both the upstream and the downstream areas of the Mekong River and the Bassac River is degraded. Bed degradation along the outer bank of the bend in the Bassac River is especially large. Sediment deposited at the entrance of the Bassac River and the south of the peninsula between the Tonle Sap River and the Mekong River. As shown in Figure 2, the peninsula between the Tonle Sap River and the Mekong River has been extended to south year by year. It is considered that the sediment deposition during the flood season cause the extension of the peninsula. As shown in Figure 8 (c), the sediment size becomes coarse at both the upstream and the downstream areas of the Mekong River and the Bassac River. Bed material in the Tonle Sap River also becomes coarse because of the inverse flow from the Mekong River. However, the armoring phenomenon is restricted near the confluence. This result gets agrees with the results of one dimensional bed deformation analysis [13].



(a) Dry season (Case 1)

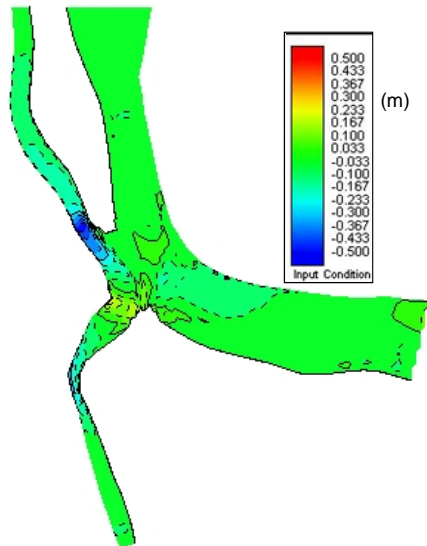


(b) Intermediate (Case 2)

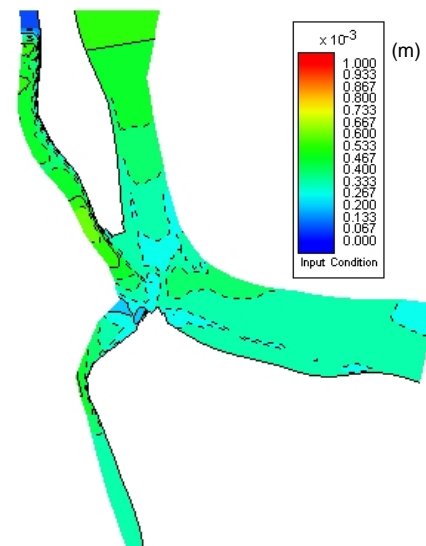


(c) Flood season (Case 3)

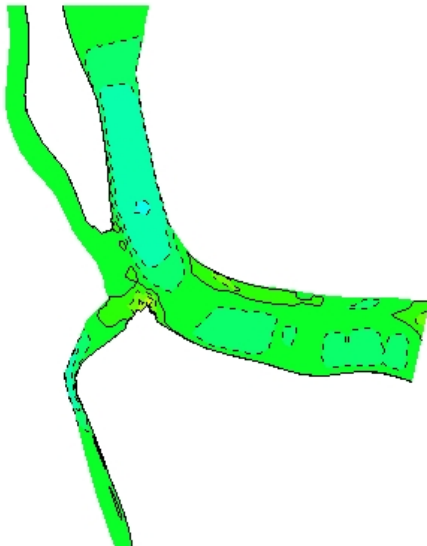
Figure 6 Depth averaged water velocity



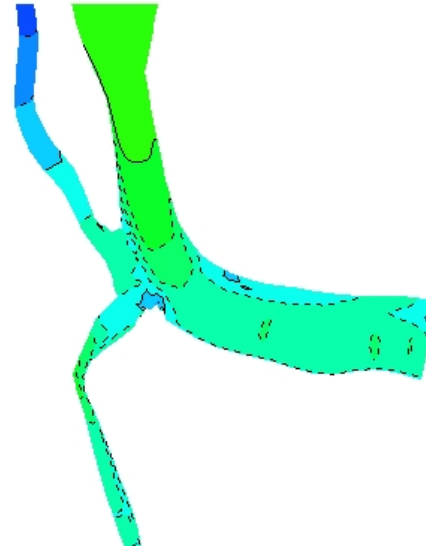
(a) Dry season



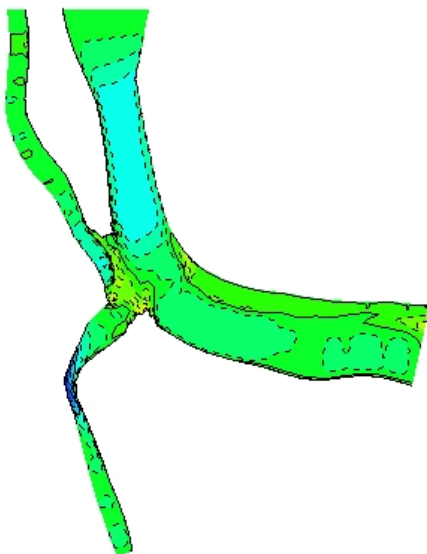
(a) Dry season



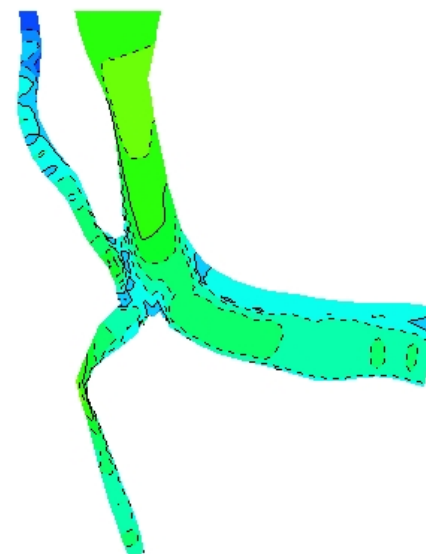
(b) Intermediate



(b) Intermediate



(c) Flood season



(c) Flood season

Figure 7 Bed deformation (Cases 1, 2 and3)

Figure 8 Mean diameter(Cases 1, 2 and3)

4.3 Effect of cohesive characteristics of the sediment on bed deformation

Figure 10 shows the bed deformation characteristics in Cases 4, 5 and 6. Both the surface and the subsurface bed materials are treated as non-cohesive material in Cases 4, 5 and 6. Comparing to the results in Cases 1, 2 and 3, the difference of the horizontal distribution of the bed deformation is quite large during the dry season (Cases 1 and 4). During the dry season (Figure 10 (a)), sediment deposited at the entrance of the Bassac River and the downstream area of the Mekong River widely, because the fine material in the Tonle Sap River is transported there very well.

When water discharge in the Tonle Sap River is equal to zero (Figure 10 (b)), the difference of the bed deformation characteristics between Case 2 and Case 5 is very small, because the water discharge in the Tonle Sap is equal to zero and no sediment transport in the Tonle Sap River.

During the flood season (Figure 10 (c)), the difference of the bed deformation characteristics between Case 3 and Case 6 is also small except for the upstream area of the Tonle Sap River. When the bed material is treated as non-cohesive material, the bed is eroded well in the upstream area of the Tonle Sap River.

As described above, cohesive characteristics of the sediment affects the bed deformation characteristics because of the suppression of sediment transport rate and bed degradation. Especially, when rivers which have different sediment size characteristics confluents, difference of the cohesive characteristics of the sediment must be considered.

5. Conclusions

The depth integrated two dimensional bed deformation analysis has been performed to understand the seasonal change of the flow pattern, bed deformation characteristics and horizontal distribution characteristics of bed material size. The obtained results are as follows.

- (1) The percentage rate of the water discharge in the Bassac River to the Mekong River is about 25% during both dry and flood seasons. However, when water discharge is equal to zero, the percentage rate of the water discharge in the

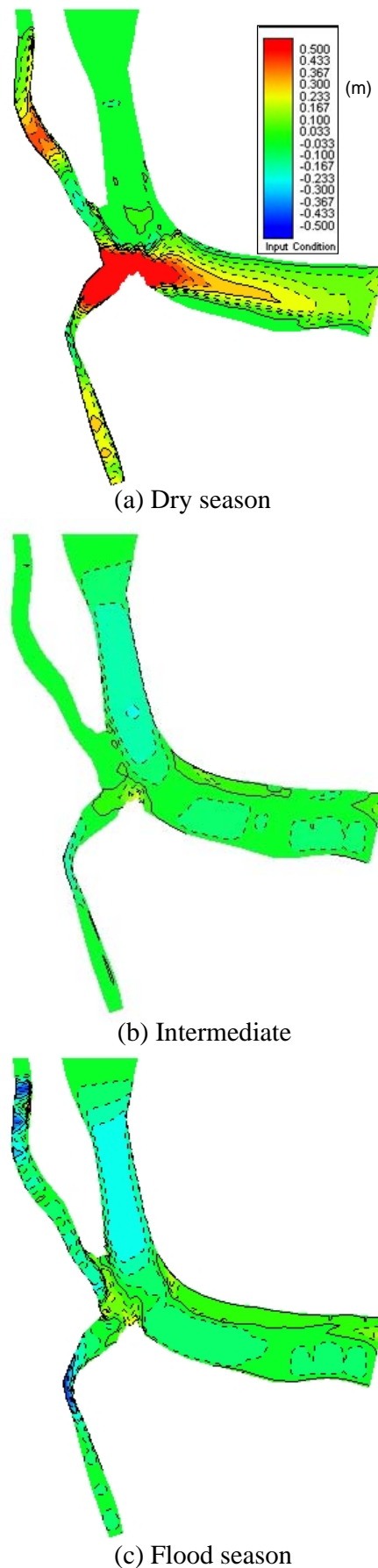


Figure 9 Bed deformation (Cases 4, 5 and 6)

Bassac River to the Mekong River becomes small.

- (2) During the flood season, sediment deposited at the south of the peninsula between the Tonle Sap River and the Mekong River. As shown in Figure 2, the peninsula between the Tonle Sap River and the Mekong River has been extended to south year by year. It is considered that the sediment deposition during the flood season cause the extension of the peninsula.
- (3) During the flood season, the bed material in the Tonle Sap River becomes coarse because of the inverse flow from the Mekong River. However, the armoring phenomenon is restricted near the confluence. These results get agrees with the results of one dimensional bed deformation analysis.
- (4) Cohesive characteristics of the sediment affects the bed deformation characteristics because of the suppression of sediment transport rate and bed degradation. Especially, when rivers which have different sediment size characteristics confluents, difference of the cohesive characteristics of the sediment must be considered.

References

- [1] Hiroshi Hori, 2000, The Mekong, Environment and Development, Kokon-Shoin Publishing Co., Ltd.
- [2] K. W. Olesen and S. Tjerry, 2002, Morphological modeling of the Chaktomuk Junction, River Flow 2002 Balkema, pp. 879-887.
- [3] Hiroshi Takebayashi, Shinji Tsukawaki, Im Sim, Touch Sambath and Sieng Sotham : Characteristics of bed deformation and size distribution of bed material at Chaktomuk in Cambodia, River Sedimentation, Vol. 11, CD-ROM version, 2010.
- [4] Luu X. Loc, Shinji Egashira and Hiroshi Takebayashi, 2004, Investigation of Tan Chau Reach in Lower Mekong Usng Field Data and Numerical Simulation, Annual Journal of Hydraulic Engineering, JSCE, Vol. 48, No.2, pp. 1057-1062.
- [5] Ashida, K. and Michiue, M. Study on hydraulic resistance and bed-load transport rate in alluvial streams, Proc. of JSCE, No. 206, pp.59-69, 1972.
- [6] Kovacs, A. and Parker, G. A new vectorial bedload formulation and its application to the time evolution of straight river channels. J. Fluid Mech. Vol. 267, pp. 153-183, 1994.
- [7] B. Y. Liu Study on Sediment Transport and Bed Evolution in Compound Channels. Thesis presented to Kyoto University, 1991.
- [8] Iwagaki, Y. Hydrodynamic study on critical shear stress. Proc. of JSCE, No. 41, pp. 1-21, 1956.
- [9] Rubey, W. W. Settling velocities of gravel, sand and silt particles, American J. of Science, Vol. 25, pp. 325-338, 1933.
- [10] Lane, E. W. and Kalinske, A. A. Engineering calculation of suspended sediment, Trans. A.G.U., Vol. 22, 1941.
- [11] Sekine, M., Nishimori, K., Fujio, K. and Katagiri, Y. On erosion process of cohesive sediment and erosion rate formula, Annual Journal of Hy. Eng. JSCE, Vol. 47, pp. 541-546, 2003.
- [12] Nagase, K. and Michiue, M. and Hinokidani O. Simulation of bed elevation around contraction in mountainous river. Annual Journal of Hy. Eng. JSCE, Vol. 40, pp. 887-892, 1996.
- [13] Hiroshi Takebayashi, Meng Chanvibol, Luu X Loc, Shinji Egashira, Shinji Tsukawaki, Im Sim, Touch Sambath and Sieng Sotham : Size Distribution of Bed and Bank Materials along The Tonle Sap River in Cambodia, Proceedings of XVth Conference of APD, pp.291-298, 2006.

(Received June 7, 2012)

異なる粘着特性の土砂を有する河川の合流部における河床変動特性

竹林洋史・プジハルサント⁽¹⁾・グエンマンミントアン⁽¹⁾・藤田正治

(1)京都大学大学院工学研究科

要 旨

カンボジア国・チャトムック地区を対象として、流れの特性、河床変動特性、河床材料の平面分布特性を明らかにするために平面二次元河床変動解析を行った。さらに、河床材料を非粘着性土と粘着性土の両方で取り扱い、粘着性土の平面分布特性が河床変動特性に与える影響を検討した。その結果、トンレサップ河とメコン河の間に形成されている半島は、洪水期の土砂の堆積により、南へ年々延伸していることが明らかとなった。さらに、粘着性土の存在は、流砂量と河床変動を抑制するため、河床変動特性に大きく影響することが明らかとなった。特に、異なる粒度を有する河川が合流するときは、粒度や粘着特性の平面分布の考慮が不可欠であることが示された。

キーワード：粘着性土，数値解析，チャトムック地区，合流